Dynamic Swelling of Tunable Full-Color Block Copolymer Photonic Gels *via* Counterion Exchange

Ho Sun Lim,[†] Jae-Hwang Lee,[†,‡] Joseph J. Walish,[†] and Edwin L. Thomas[†,‡,*]

[†]Department of Materials Science and Engineering, Institute for Soldier Nanotechnologies, Massachusetts Institute of Technology, Cambridge, Massachusetts 02139, United States and [‡]Department of Mechanical Engineering and Materials Science, Rice University, Houston, Texas 77251, United States

ABSTRACT

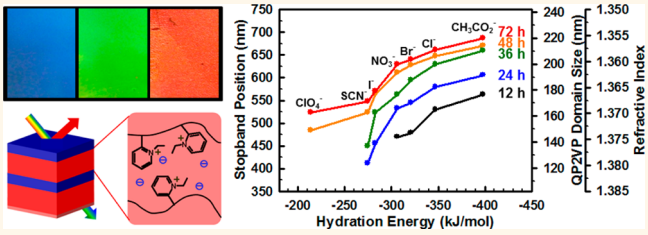

One-dimensionally periodic block copolymer photonic lamellar gels with full-color tunability as a result of a direct exchange of counteranions were fabricated *via* a two-step procedure comprising the self-assembly of a hydrophobic block—hydrophilic polyelectrolyte block copolymer, polystyrene-*b*-poly(2-vinyl pyridine) (PS-*b*-P2VP), followed by sequential quaternization of the P2VP layers in 1-bromoethane solution. Depending on the hydration characteristics of each counteranion, the selective swelling of the block copolymer lamellar structures leads to large tunability of the photonic stop band from blue to red wavelengths. More extensive quaternization of the P2VP block allows the photonic lamellar gels to swell more and red shift to longer wavelength. Here, we investigate the dynamic swelling behavior in the photonic gel films through time-resolved *in situ* measurement of UV—vis transmission. We model the swelling behavior using the transfer matrix method based on the experimentally observed reflectivity data with substitution of appropriate counterions. These tunable structural color materials may be attractive for numerous applications such as high-contrast displays without using a backlight, color filters, and optical mirrors for flexible lasing.

KEYWORDS: block copolymer lamellar gels · dynamic swelling · ion exchange · tunable color · photonic band gap

A number of biological organisms have hierarchical micro- and nanotextures, which play an important role in controlling their body color, helping prevent predators from tracking.[1−4] The skin of some fish, reptiles, and amphibians has complex optical microstructures that are composed of stacks of alternating layers of cytoplasm and reflectin proteins with low and high refractive index, respectively, producing strong reflective iridescent colors. The dorsal mantle of certain cephalopods exhibits brilliant structural colors primarily due to changes in thickness of the platelets arising from swelling due to local secretion of chemicals from neurotransmitters. Clearly, nature provides an awesome inspiration for the design of structured color materials.

Block copolymers (BCPs) with well-defined periodic nanoscale features have been employed to develop materials having photonic band gaps (PBGs), frequency ranges of light being reflected, due to their spontaneous self-assembly into long-range-ordered microstrctures.[5,6] Block copolymers provide a fascinating material platform for creating various 1D, 2D, and 3D photonic crystals, which can be manipulated by changing both domain spacing and refractive index contrast.[7−9] Although the typical domain size of lamellae in self-assembled BCPs in the case of typical molecular weight (~50 kg/mol) is insufficient to exhibit a PBG in the visible spectrum, the expansion of the lamellar period by contact with water or other solvents can yield a strong reflective color.[10,11] In particular, the use of BCPs with stimuli-responsive units allows photonic gels to have large tunability of the PBG.[12−17]

In this study, we present the dynamic swelling behavior of a photonic lamellar gel made of a hydrophobic block—hydrophilic polyelectrolyte block copolymer with full-color tunability by selection of the proper counterions. Polyelectrolytes undergo changes in their chain dimension upon exchange of counteranions, in response to the large changes in solubility in aqueous solution depending on the hydration nature of the counterions (Figure 1).[17−19] We also model the swelling behavior using the transfer matrix method based on the experimentally observed reflectivity data with substitution of appropriate counterions.

* Address correspondence to elt@rice.edu.

Received for review July 2, 2012 and accepted September 28, 2012.

Published online September 28, 2012
10.1021/nn302949n

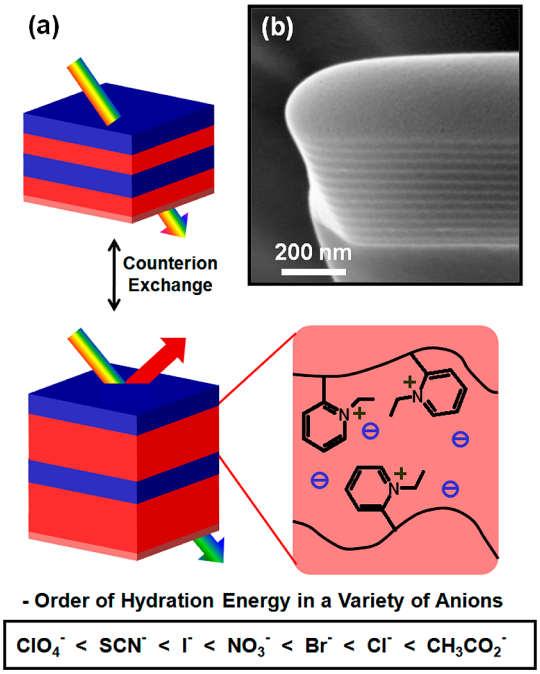

Figure 1. (a) Schematic representation of the mechanism for color change in the PS-*b*-QP2VP photonic lamellar gels by a direct exchange of counterions. Depending on the hydration characteristics of the counteranions, the selective swelling in the block copolymer lamellar structures can be controlled, causing a change in the optical properties. When the QP2VP block is coordinated with anions of high hydration energy, the block copolymer lamellar structures swell to a greater extent when in contact with a water reservoir, leading the reflected light to red shift to longer wavelengths. (b) Cross-sectional SEM image (52° tilt) of a focused ion beam milled dry PS-*b*-QP2VP lamellar film. To enhance the layer contrast, the films were exposed to iodine vapor for a selective staining of the QP2VP layers, resulting in brighter layers.

RESULTS AND DISCUSSION

Tunable BCP photonic gels were fabricated from well-ordered polystyrene/poly(2-vinylpyridine) (PS/P2VP) lamellar structures with the total (dry) film thickness of about 1 μm (about 20 periods of the diblock) with subsequent quaternization of the P2VP layers (denoted QP2VP). Initially, lamellar PS-*b*-P2VP films were prepared by spin-casting from 5 wt % solution of PS-*b*-P2VP (M_n = 57 kg/mol-*b*-57 kg/mol) in propylene glycol monomethyl ether acetate onto an iodosilane-treated glass substrate and subsequently annealed in an atmosphere of chloroform vapor at 50 °C for 24 h. Films cast onto untreated substrates would, after long periods of time, sometimes delaminate owing to the high degree of swelling of the P2VP block. This delamination of the film from the substrate did not regularly occur during the course of the experiments; however, the iodosilane treatments were used for experimental consistency with previous work.[12,14] Additionally, intrafilm delamination does not seem to occur and is thought to be the result of "physical cross-links" introduced by

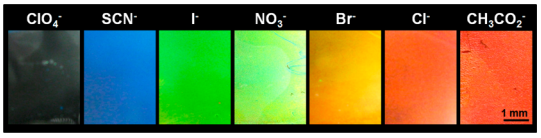

Figure 2. Color change of the photonic gel films quaternized for 36 h with direct exchange of counteranions. The color of the photonic gel films shifts from transparent to blue, green, and red with increasing hydration energy of the counteranions. The photographs were taken on a black background under fluorescent lights, and the counterions were exchanged using 10 mM solution of a variety of tetrabutylammonium salts.

numerous screw dislocations in the lamellar structure. As a result, the PBG changes of the BCP gels were reversible without incurring significant damage even after several tens of exchange cycles. Quaternizing of the P2VP layers was done by a mixture of 1-bromoethane and hexane at 50 °C for predetermined times, leading to the conversion of pyridine rings into pyridinium groups.[12] As a result, the PS-*b*-QP2VP lamellar films swell when exposed to a reservoir of aqueous solvent.

Since the domain thicknesses of the dry photonic gel films are not sufficiently large to exhibit a PBG in the visible region, the dry films are transparent. The internal structures of dry photonic gels were confirmed by scanning electron microscopy (SEM) (Figure 1b). The photonic films were exposed to iodine (I_2) vapor to enhance secondary electron contrast due to a selective staining of the QP2VP layers and then cut using a focused ion beam (FIB) for cross-sectional imaging.[20] A well-ordered parallel lamellar morphology was observed in the PS-*b*-QP2VP film with the average dry periodicity of about 48 nm. The bright and dark regions in Figure 1b correspond, respectively, to the I_2-stained QP2VP lamellar domains and the unstained PS domains. The two types of domains have nearly identical layer thicknesses, as expected from the symmetric composition of the BCP. The lamellae were oriented parallel to the glass substrate due to the preferential interaction of the P2VP block with the glass substrate. When swollen, the parallel multilayered lamellar stacks selectively reflect light with specific wavelengths according to Bragg diffraction.[21]

Upon immersion into a water reservoir, the films immediately display visible structural color from strong specific reflection due to the selective swelling of the hydrophilic QP2VP block. As the hydrophilic QP2VP blocks swell, the glassy hydrophobic PS layers resist in-plane expansion and only allow anisotropic expansion of the QP2VP layers along the normal direction to the layers, leading to an increase in both QP2VP domain thickness and refractive index contrast.[12] Figure 2 shows the observed range of structural colors taken imaged under fluorescent lights on a black background of a photonic gel quaternized for 36 h. The as-prepared photonic gel film displayed a distinctive

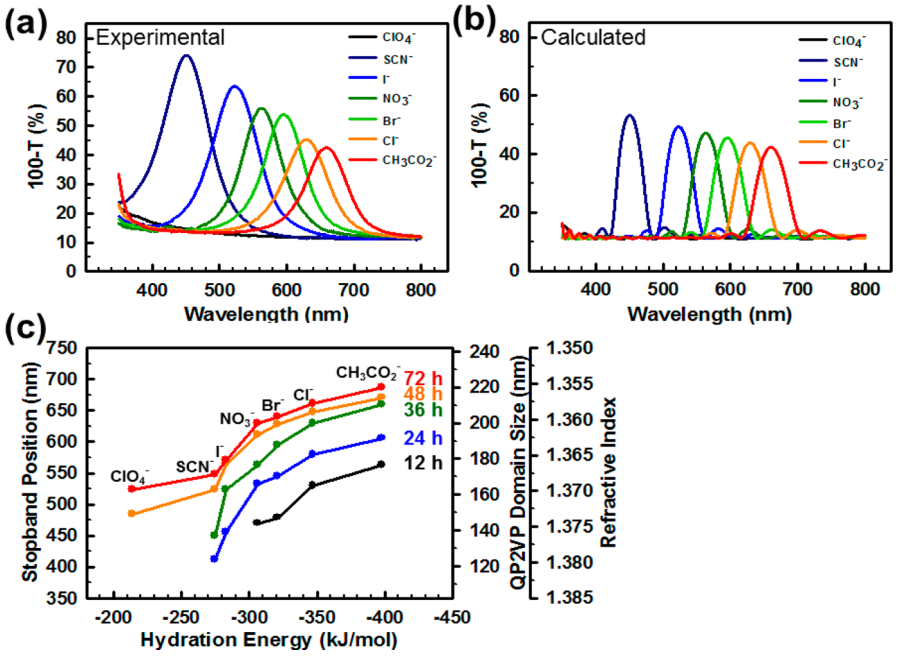

Figure 3. (a) Reflectivity spectra of the PS-*b*-QP2VP photonic gels as a result of direct ion exchange. (b) Simulated reflectivity spectra by TMM calculations of the photonic lamellar films. Differences between the experimental and calculated results are mainly attributed to the many defects in the lamellar structure. (c) Changes in the photonic stop band position, the QP2VP lamellar domain thickness, and refractive index of the tunable PS-*b*-QP2VP photonic gels as a function of the hydration energy of the counteranions.

orange color, resulting from the coordination of the QP2VP units with Br^- anions having high hydration affinity. The color of the BCP photonic gels can be easily modulated through directly exchanging counteranions possessing a variety of hydration characteristics. When the Br^- counteranions were replaced with SCN^-, I^-, NO_3^-, Cl^-, and $CH_3CO_2^-$, the color of the BCP gel could be controlled from blue to red, while replacing Br^- with ClO_4^- resulted in no visible color on the photonic gels since, in this instance, the layer period is insufficient to show a reflection in the visible regime. The polyelectrolyte photonic gel films have distinct RGB colors: when QP2VP layers were coordinated with Cl^- (red), I^- (green), and SCN^- (blue), their RGB values were (238, 95, 55), (81, 218, 51), and (58, 124, 218) for Cl^-, I^-, and SCN^- ions, respectively. This is attributed to the volume changes in the quaternized hydrophilic block layers, which strongly depend on the hydration nature of the anions and intimately relate with the effective hydrophilicity of the QP2VP block coordinated with the particular anions. The specific ion-pairing interactions induce a large change in the chemical component of QP2VP layers and thus changes in domain spacing (primarily) and refractive index (secondarily), thereby directly influencing the optical properties of the dielectric multilayered stack. When the different anions were repeatedly replaced *via* consecutive counteranion exchanges, the tunability of the optical properties was reversible up to several tens of switching cycles.

The changes of the stop band in the photonic gel films were monitored by measuring reflectivity with variation of ion-pairing interaction. Since the absorption of the film is negligible, the sum total of the reflectivity and the transmission is approximately 100%. The reflection maxima (λ_{max}) represent the PBG positions and correlate with the distinctive structural colors. Figure 3a shows UV–vis reflection spectra of the photonic lamellar gels as a function of the type of counteranion. As the coordinated counteranions exchange from Br^- to SCN^-, I^-, NO_3^-, Cl^-, and $CH_3CO_2^-$, the primary PBG position shifts from approximately 595 to 450, 535, 565, 630, and 660 nm, respectively. The continuous shifting of the PBG is attributed primarily to the change in the thickness of the QP2VP layers. As shown in Figures 2 and 3, the films containing anions with a smaller hydration degree than ClO_4^- ions were transparent to the naked eye. On the other hand, exchange with counterions having a higher hydration energy leads to a red shift of the PBG to longer wavelengths, displaying an intense structural color as the QP2VP gel layers expand. The order of surface hydrophobicity of polyelectrolyte brushes with various counterions is $C_7F_{15}CO_2^- > C_3F_7CO_2^- > PF_6^- > ClO_4^- > SCN^- > I^- > NO_3^- > Br^- > Cl^- > F^- > CH_3CO_2^-$.[19,22] The swelling behavior of our 1D photonic gel films is in good agreement with this trend in wetting behavior found for polyelectrolyte brush-modified substrates.

We modeled the swelling behavior using the transfer matrix method (TMM), assuming a structure composed of 20 periods of parallel lamellae (Figure 3).[23] The wavelength corresponding to the maximum reflectivity strongly depends on the domain spacings

and refractive indices of each block, while the peak intensity is determined by the number of periods of the dielectric structures and the refractive index contrast. By normalizing the intensity to the film swollen with $CH_3CO_2^-$, the calculated reflectance spectra correspond quite well to the experimentally measured spectra. (compare Figure 3a,b). The decrease in peak intensity with increasing hydration energy is attributed to the large mismatch in optical thickness ($n_1 \cdot d_1$ *vs* $n_2 \cdot d_2$) between the QP2VP and PS layers which increases with further swelling of the QP2VP layers (Figure S5 in Supporting Information). Ideally, the strongest reflectivity of a 1D dielectric structure occurs for a quarter wave stack. Since the optical path length of the dry glassy PS layers is unchanged during swelling, the efficiency of reflectivity decreases as a result of swelling. The experimentally measured spectra are broader than the calculated reflectance spectra, which assume perfectly flat, parallel layers. The broadening results from the microstructural defects such as pores and screw dislocations (see Figure S1).[12,13]

The photonic stop band can be also modulated with the degree of quaternization of the P2VP block, which affects the hydration properties. The increase of degree of ionization in the QP2VP layers magnifies the hydrophilicity, as the change in charge density of the polyelectrolyte gels affects the free energy related with the mixing of the polyelectrolyte blocks and the water molecules. Figure S2 shows the reflectivity spectra of the photonic gels with different degrees of quaternization, in contact with various counteranion solutions. As expected, the more highly quaternized photonic films have a larger red shift, resulting from more swelling of the higher charge density QP2VP layers (Figure S3). Figure 3c plots the shift of the PBG as a function of quaternization time for various anions. Thus the balance between the degree of ionization and the hydration energy effectively governs the swelling behavior in the photonic gels.

As shown in Figure 2, the swelling of photonic gels transforms a specific anion binding into a visual signal upon direct ion exchange. We can create a photonic sensor by using an array of films with different degrees of quaternization. For example, in the case of the photonic gel films quaternized for 36 h, the structural colors are clearly distinctive: yellow for Br^- and red for Cl^- ions.

In order to more quantitatively analyze the swelling behavior of the photonic gel films with direct ion exchange, we calculated the domain size in each state based on the measured reflectivity spectra *via* TMM. The TMM calculations can provide information on the lamellar domain size and the refractive indices and the volume fraction of liquid in the QP2VP block layers. The original spacings of the PS and QP2VP block layers were both 24 nm (measured from TEM micrographs). On the basis of the TMM calculations, the domain thickness of the QP2VP layers varied from 24 to 220 nm depending on the degree of quaternization of the P2VP block and the hydration energy of the particular coordinated counteranions (Table S1). Figure 3c shows the thickness and refractive index change of QP2VP domains as a function of hydration energy of counterions. For example, for the photonic gels quaternized for 36 h, the calculated thickness of the QP2VP lamellar domains increased from 24 nm for the dry state to 135, 163, 178, 190, 202, and 214 nm for aqueous solutions with SCN^-, I^-, NO_3^-, Br^-, Cl^-, and $CH_3CO_2^-$ ions, respectively. The selective swelling of the QP2VP layers leads to a thickness increase of the QP2VP layers of up to nearly 900% relative to the dry films, with a commensurate shift of the optical stop band toward longer wavelengths.

We have also investigated the dynamics of the swelling of the photonic lamellar gels through time-dependent measurements of the UV–vis transmission (Figure 4). As shown in Figure 4a, a film initially rapidly takes up water, reaching near-equilibrium in a few seconds. For example, starting with a dry film, the broad reflectance peak centered at around 530 nm for the swollen photonic film with Br^- ions started to appear within 0.15 s and then continuously red-shifted, approaching the final peak position of 595 nm after about 1 s (Figure 4c). The intensity of reflectance abruptly increased upon a contact with water and gradually saturated to around 45% in the final stage. The early occurrence of a low intensity and broad reflectance peak implies that the lamellar gels swell inhomogeneously, most likely from the outermost surface inward. On the basis of the TMM calculations, the lamellar structures mostly swell at the beginning since the QP2VP lamellar domains must expand up to greater than 6.5 times (from 24 to 165 nm) to exhibit the reflectivity maximum at 530 nm. Other ions showed similar dynamic swelling behavior (see Figure S4). Figure 4d shows the response times as a function of hydration characteristics of the various counteranions. The time to swell the photonic gels decreased from about 4.1 s for SCN^- to about 1.1 s for Cl^- ions, demonstrating that a greater driving force accelerates both the swelling kinetics and extent of swelling.

The time-dependent reflectance spectra are simulated by TMM (Figure 5). The model assumes 15 pairs of PS and QP2VP layers, with each type of layer of the same initial thicknesses and initial refractive index: 24 nm and 1.6. Upon contacting the aqueous solution ($n \sim 1.33$), the P2VP layer swells *via* diffusion of the solution. The liquid volume fraction in the QP2VP layers is modeled by a Gaussian function, $f_V(z,t) = f_M \exp(-z^2/4Dt)$, where the saturation volume fraction (f_M) and diffusion coefficient (D) can be chosen to reflect the experimental results. Figure S6 displays simulated reflectance results to justify these parameters. The effective refractive index and swollen thickness of the P2VP layers are

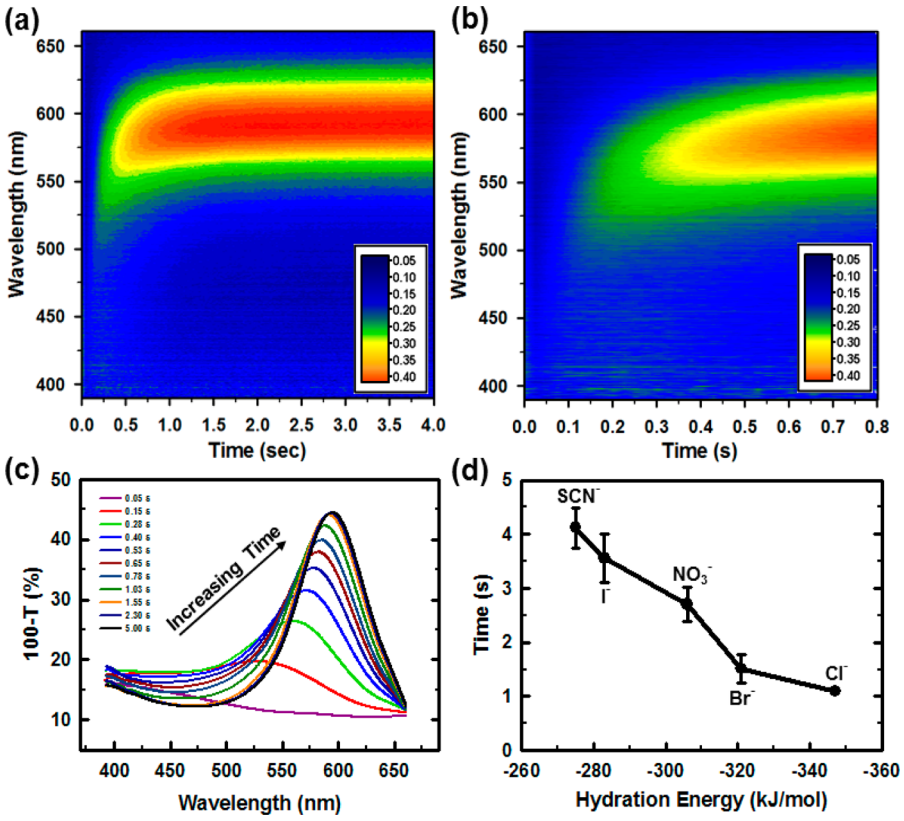

Figure 4. Dynamic swelling behavior of PS-*b*-QP2VP film exposed to aqueous Br^- solution. (a,b) Plot of experimental reflectivity *versus* time. (b) Short time behavior and (c) related UV–visible spectra obtained by plotting intensity *vs* wavelength at various times during swelling. Note the appearance of a broad initial peak, which grows in intensity, narrows, and red shifts with increased swelling time. (d) Time required to swell the QP2VP lamellar domains as a function of hydration energy of counteranions.

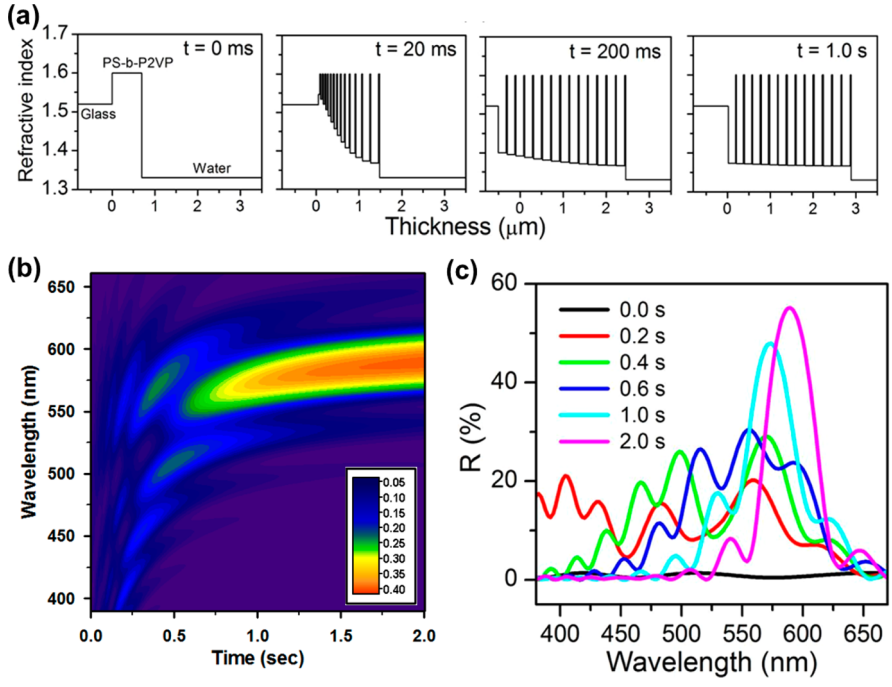

Figure 5. Simulated dynamic swelling behavior of PS-*b*-QP2VP film exposed to aqueous Br^- solution. (a) Reflectance profiles at four selected time frames. (b) Calculated reflectance spectra map and (c) reflectance spectra at six different time frames. In the simulation, the diffusion coefficient and the saturation volume fraction are 4×10^{-8} cm^2/s and 0.876.

given by $n_{eff} = (n^2_{P2VP} - f_V(n^2_{P2VP} - n^2_{water}))^{1/2}$ and $d = d_0/(1 - f_V)$. Figure 5a shows a time evolution of index profiles due to the diffusion of water into the P2VP layers. The reflectance map (Figure 5b), calculated by the time-dependent profile of refractive indices, shows the absence of the major reflection peak at the initial swelling period, which agrees with the experimental observation in Figure 4. The index profile at 200 ms looks similar to the final profile, and this index profile does not create the main reflection peak due to the lack of constructive interference in a chirped structure. At 600 ms after water contact (Figure 5c), the corresponding refractive index profile is close to the saturated profile. As a result, the characteristic reflection peak in the model appears abruptly and near the final peak position rather than sweeping in from a shorter wavelength as is evident in the experimental results. The oscillatory features appearing in every simulated spectrum are not observed in the experimental spectra in Figure 4 likely due to the spectral smoothing from inhomogeneous local swelling speeds, a range of acceptance angles in the actual measurements, and a finite interface width between domains due to some intermixing in the real sample. However, the simulation results quantitatively confirm the successive swelling of the P2VP layers and suggest that importance of diffusion engineering for faster response time of photonic gels.

CONCLUSION

We have demonstrated full-color tunability of variously quaternized polystyrene−poly(2-vinyl pyridine) block copolymer films *via* selection of appropriate anions. The position of the PBG of the photonic gel films could be managed by choice of the hydration characteristics of the counteranions and the degree of quaternization of the QP2VP microdomains. The selective swelling of the block copolymer lamellar structure with various ions allows tunability of the film from transparent to blue to red depending on the hydration strength of the ions. These results provide useful information for understanding the dynamic swelling behavior of the photonic lamellar gels with distinctive structural RGB color and suggest the ability to design color sensors and multiband filters.[24]

METHODS

Materials. Polystyrene-*b*-poly(2-vinyl pyridine) (PS-*b*-P2VP) block copolymer with a number average molecular weight of 57 PS−57 P2VP kg/mol was used as received from Polymer Source, Inc. (Dorval, Canada). All chemicals were purchased from Sigma-Aldrich Co. LLC (Milwaukee, WI) and used without further purification.

Preparation of Photonic Gel Films. PS-*b*-P2VP block copolymer was dissolved in propylene glycol monomethyl ether acetate (PGMEA) to make a 5% solution by weight. After dissolution, a 0.2 μm syringe filter was used to remove any particulate contaminants, and the solution was degassed in a vacuum oven prior to spin-coating. Glass slides were first treated with (3-aminopropyl)triethoxysilane or (3-iodopropyl)trimethoxysilane as an adhesion promoter to ensure that the films did not delaminate from the substrate after immersion into the aqueous solution. Substrates were prepared using an open vial of the adhesion promoter placed in a vacuum desiccator along with the glass slides. Vacuum was applied for 10 min, the vacuum connection was closed, and the slides were allowed to sit for 5 min. The slides were then used for spin-coating within the next 15 min. The 5% PS-*b*-P2VP solution was uniformly distributed across the surface of the functionalized glass slides and then spun at 500 rpm for 90 s. After spin-coating, samples were suspended above chloroform in a jar with a loose fitting lid to avoid condensation, and the jar was maintained at 50 °C on a hot plate for 24 h. Upon completing the chloroform vapor annealing treatment, P2VP layers were quaternized by immersing the films in 10 vol % hexane solution of 1-bromoethane at 50 °C for various times. To exchange the counterions, the quaternized photonic gel films were immersed in a 10 mM solution of a variety of tetrabutylammonium salts of the appropriate counterions for a certain time.

Characterizations. A cross-sectional image of the block copolymer lamellar structures was obtained by scanning electron microscopy after milling by a focused ion beam. Ultraviolet−visible spectra were investigated on a Varian Cary 6000i in transmission mode. Photographs were taken on black background under fluorescent light. Time-dependent reflectivity was measured with a fiber optic spectrometer (Ocean Optics HR 4000) in transmission mode with an interval between successive spectra of 25 ms *in situ*. A water droplet was placed near an area to be detected, then a glass slide covered the drop, rapidly pushing the solution across the area being monitored by the spectrometer.

Conflict of Interest: The authors declare no competing financial interest.

Acknowledgment. The work was supported by the grant funded by the U.S. Army Research Office under contract W911NF-07-D-0004 and the U.S. Air Force under Grant AOARO 114095, United States and the Korea Research Foundation Grant funded by the Korean Government (KRF-2008-357-D00069), Korea.

Supporting Information Available: Detailed information on characterizations. This material is available free of charge *via* the Internet at http://pubs.acs.org.

REFERENCES AND NOTES

1. Mathger, L. M.; Land, M. F.; Siebeck, U. E.; Marshall, N. J. Rapid Colour Changes in Multilayer Reflecting Stripes in the Paradise Whiptail, *Pentapodus paradiseus*. *J. Exp. Biol.* **2003**, *206*, 3607–3613.
2. Hanlon, R. Cephalopod Dynamic Camouflage. *Curr. Biol.* **2007**, *17*, R400–R404.
3. Kasukawa, H.; Oshima, N.; Fujii, R. Control of Chromatophore Movements in Dermal Chromatic Units of Blue Damselfish. 2. The Motile Iridophore. *Comp. Biochem. Physiol., Part C: Toxicol. Pharmacol.* **1986**, *83*, 1–7.
4. Parker, A. R.; Townley, H. E. Biomimetics of Photonic Nanostructures. *Nat. Nanotechnol.* **2007**, *2*, 347–353.
5. Park, C.; Yoon, J.; Thomas, E. L. Enabling Nanotechnology with Self-Assembled Block Copolymer Patterns. *Polymer* **2003**, *44*, 6725–6760.
6. Lodge, T. P. Block Copolymers: Past Successes and Future Challenges. *Macromol. Chem. Phys.* **2003**, *204*, 265–273.
7. Urbas, A.; Sharp, R.; Fink, Y.; Thomas, E. L.; Xenidou, M.; Fetters, L. J. Tunable Block Copolymer/Homopolymer Photonic Crystals. *Adv. Mater.* **2000**, *12*, 812–814.
8. Deng, T.; Chen, C. T.; Honeker, C.; Thomas, E. L. Two-Dimensional Block Copolymer Photonic Crystals. *Polymer* **2003**, *44*, 6549–6553.

9. Urbas, A. M.; Maldovan, M.; DeRege, P.; Thomas, E. L. Bicontinuous Cubic Block Copolymer Photonic Crystals. *Adv. Mater.* **2002**, *14*, 1850–1853.
10. Yoon, J.; Lee, W.; Thomas, E. L. Thermochromic Block Copolymer Photonic Gel. *Macromolecules* **2008**, *41*, 4582–4584.
11. Edrington, A. C.; Urbas, A. M.; DeRege, P.; Chen, C. X.; Swager, T. M.; Hadjichristidis, N.; Xenidou, M.; Fetters, L. J.; Joannopoulos, J. D.; Fink, Y.; *et al.* Polymer-Based Photonic Crystals. *Adv. Mater.* **2001**, *13*, 421–425.
12. Kang, Y.; Walish, J. J.; Gorishnyy, T.; Thomas, E. L. Broad-Wavelength-Range Chemically Tunable Block-Copolymer Photonic Gels. *Nat. Mater.* **2007**, *6*, 957–960.
13. Lee, W.; Yoon, J.; Lee, H.; Thomas, E. L. Direct 3-D Imaging of the Evolution of Block Copolymer Microstructures Using Laser Scanning Confocal Microscopy. *Macromolecules* **2007**, *40*, 6021–6024.
14. Walish, J. J.; Kang, Y.; Mickiewicz, R. A.; Thomas, E. L. Bioinspired Electrochemically Tunable Block Copolymer Full Color Pixels. *Adv. Mater.* **2009**, *21*, 3078–3081.
15. Kim, E.; Kang, C.; Baek, H.; Hwang, K.; Kwak, D.; Lee, E.; Kang, Y.; Thomas, E. L. Control of Optical Hysteresis in Block Copolymer Photonic Gels: A Step towards Wet Photonic Memory Films. *Adv. Funct. Mater.* **2010**, *20*, 1728–1732.
16. Chan, E. P.; Walish, J. J.; Thomas, E. L.; Stafford, C. M. Block Copolymer Photonic Gel for Mechanochromic Sensing. *Adv. Mater.* **2011**, *23*, 4702–4706.
17. Ahn, Y.; Kim, E.; Hyon, J.; Kang, C.; Kang, Y. Photoresponsive Block Copolymer Photonic Gels with Widely Tunable Photosensitivity by Counter-Ions. *Adv. Mater.* **2012**, *23*, OP127–OP130.
18. Azzaroni, O.; Moya, S.; Farhan, T.; Brown, A. A.; Huck, W. T. S. Switching the Properties of Polyelectrolyte Brushes *via* "Hydrophobic Collapse". *Macromolecules* **2005**, *38*, 10192–10199.
19. Azzaroni, O.; Brown, A. A.; Huck, W. T. S. Tunable Wettability by Clicking into Polyelectrolyte Brushes. *Adv. Mater.* **2007**, *19*, 151–154.
20. Kim, B. J.; Kang, H. M.; Char, K.; Katsov, K.; Fredrickson, G. H.; Kramer, E. J. Interfacial Roughening Induced by the Reaction of End-Functionalized Polymers at a PS/P2VP Interface: Quantitative Analysis by DSIMS. *Macromolecules* **2005**, *38*, 6106–6114.
21. Bonifacio, L. D.; Lotsch, B. V.; Puzzo, D. P.; Scotognella, F.; Ozin, G. A. Stacking the Nanochemistry Deck: Structural and Compositional Diversity in One-Dimensional Photonic Crystals. *Adv. Mater.* **2009**, *21*, 1641–1646.
22. Lim, H. S.; Lee, S. G.; Lee, D. H.; Lee, D. Y.; Lee, S.; Cho, K. Superhydrophobic to Superhydrophilic Wetting Transition with Programmable Ion-Pairing Interaction. *Adv. Mater.* **2008**, *20*, 4438–4441.
23. Pendry, J. B.; Mackinnon, A. Calculation of Photon Dispersion-Relations. *Phys. Rev. Lett.* **1992**, *69*, 2772–2775.
24. Arsenault, A. C.; Puzzo, D. P.; Manners, I.; Ozin, G. A. Photonic-Crystal Full-Colour Displays. *Nat. Photonics* **2007**, *1*, 468–472.